Photophysical Properties of Kuratowski-Type Coordination Compounds $[M^{II}Zn_4Cl_4(Me_2bta)_6]$ (M^{II} = Zn or Ru) Featuring Long-Lived Excited Electronic States

Ying-Ya Liu,[a] Maciej Grzywa,[a] Markus Tonigold,[a] German Sastre,*[,b] Tanja Schüttrigkeit,[c] Nicholas S. Leeson,[d] and Dirk Volkmer*[a,e]

[a] *Ulm University, Institute of Inorganic Chemistry II - Materials and Catalysis, Albert-Einstein-Allee 11, D-89081 Ulm, Germany.*
[b] *Instituto de Tecnologia Quimica (UPV-CSIC),Universidad Politecnica de Valencia , Av. Los Naranjos s/n, 46022 Valencia, Spain*
[c] *Hamamatsu Photonics Deutschland GmbH, Arzbergerstraße 10, D-82211 Herrsching, Germany*
[d] *Edinburgh Instruments Ltd, 2 Bain Square, Kirkton Campus, Livingston, EH54 7DQ, UK.*
[e] *Augsburg University, Institute of Physics, Chair of Solid State and Material Science, Universitätsstr. 1, D-86159 Augsburg, Germany.*
Fax: +49 (821) 598-5955; Tel: +49 (821) 598-3006; E-mail: dirk.volkmer@physik.uni-augsburg.de

Contents

Fig. S12. Main components of the two bands in the UV-Vis spectrum of compound **3**, $[Zn_5Cl_4(ta)_6]$ (cf. Fig. 11 in the manuscript). 'f' is the oscillator strength. The bands at 284 and 233 nm are of LLCT type.

Fig. S13. Main components of the two bands in the UV-Vis spectrum of **3-Ru**, $[RuZn_4Cl_4(ta)_6]$ (cf. Fig. 11 in the manuscript). 'f' is the oscillator strength. The bands at 357 and 328 nm are of d-d and MLCT type whereas the band at 276 nm is a LLCT involving the Cl^- ligands.

Table S1. UV/Vis and steady-state fluorescence spectroscopic data of the three compounds.

Fig. S14. DFT (HCTH-TZVPP) calculated infrared spectrum of (**3**). Compare to **Fig. S8.** The main features are: 815 (CH out of plane), 978 (ta skeleton, CCN bending), 1138 (HCN bending), 1222 (ZnN asym. stretching), 1448 (CN stretching or HCN bending), 1485 (C=C stretching) and 3245 (CH stretching).

Fig. S15. DFT (HCTH-TZVPP) calculated Raman spectrum of (**3**), which gives as main active bands: 1011 (HCN bending), 1226 (ZnN stretching), 1281 (CN stretching), 1486 (CC stretching) and 3263 (CH stretching). Compare to **Fig. S9**.

Fig. S16. Comparative features of DFT (HCTH-TZVPP) calculated infrared spectra of compounds **1**, **3** and **3-Ru**.

Fig. S17. Comparative features of DFT (HCTH-TZVPP) calculated infrared spectra of compounds **3** and **3-Ru**.

Table S2. Active normal vibrational modes in the infrared spectra of compounds **3** and **3-Ru**, as calculated from DFT (HCTH-TZVPP). See **Figs. S16** and **S17**.

Fig. S18. Fluorescence excitation spectra of Me_2btaH in acetonitrile solution (—) and acetonitrile reference (····).

Fig. S19. Raman signals swamping the emission spectra of compound **1** (light blue, $\lambda_{EXC.}$=284nm, dark blue, $\lambda_{EXC.}$=280nm).

Fig. S20. TRES (Time Resolved Emission Spectrum) of **1**, $\lambda_{EXC.}$ = 273nm.

Fig. S21. Steady-state emission (▲,$\lambda_{EXC.}$=250 nm) and quasi-steady-state (△,λ_{EXC}=273 nm) spectra of compound **1**.

Fig. S22. Steady-state spectra of acetonitrile ($\lambda_{EXC.}$=335 nm, ····), **1** in acetonitrile, ($\lambda_{EXC.}$=330, ----), **1** in acetonitrile ($\lambda_{EXC.}$= 330 nm, —).

Fig. S23. Kinetic scan of **1** (black), **2** (light grey) and Me_2btaH (dark grey).

Fig. S24. Fluorescence decays of Me_2btaH (top), **1** (middle) and **2** (bottom) before (□) and after (△) photobleaching. IRF (—), Fit (—), $\lambda_{EXC.}$=280nm.

Table S3. Experimental conditions of steady-state and lifetime measurements of **1**.

Table S4. Experimental conditions of steady state and lifetime measurements of **2**.

Table S5. Experimental conditions of all steady state measurements of Me_2btaH.

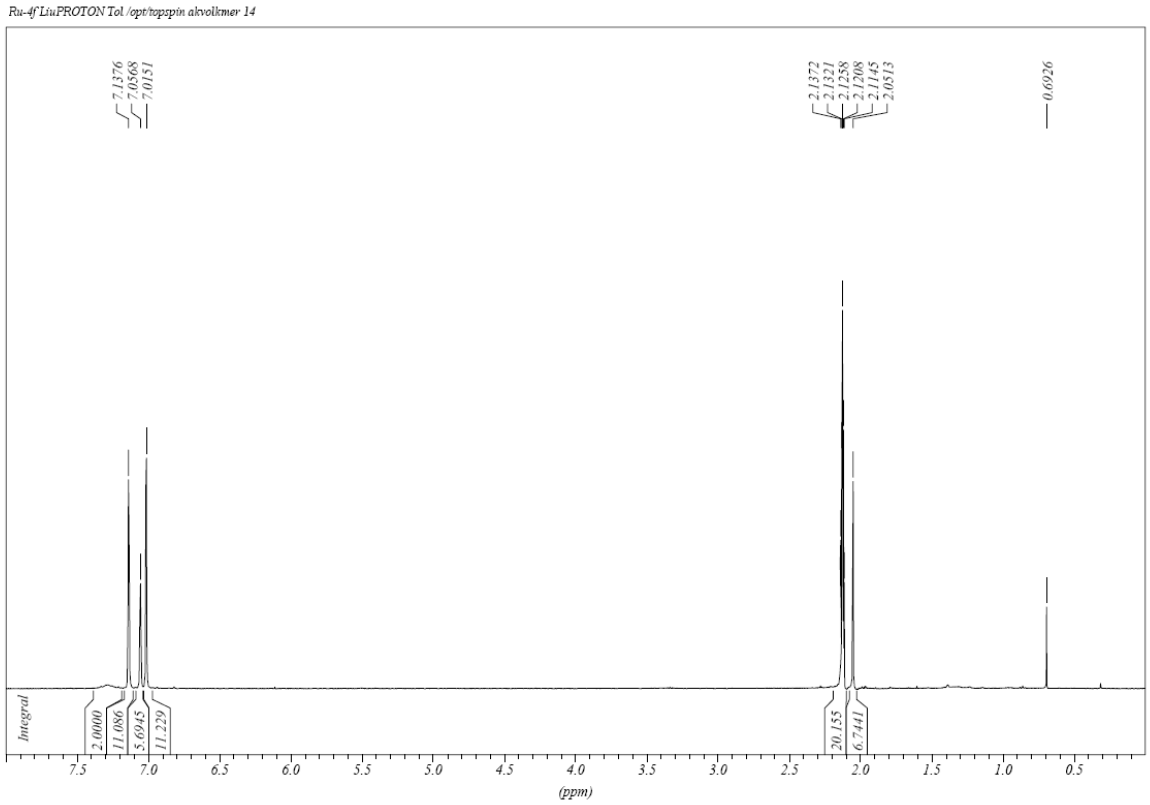

Fig. S1. ^{1}H-NMR of **2** in toluene-d^{8}.

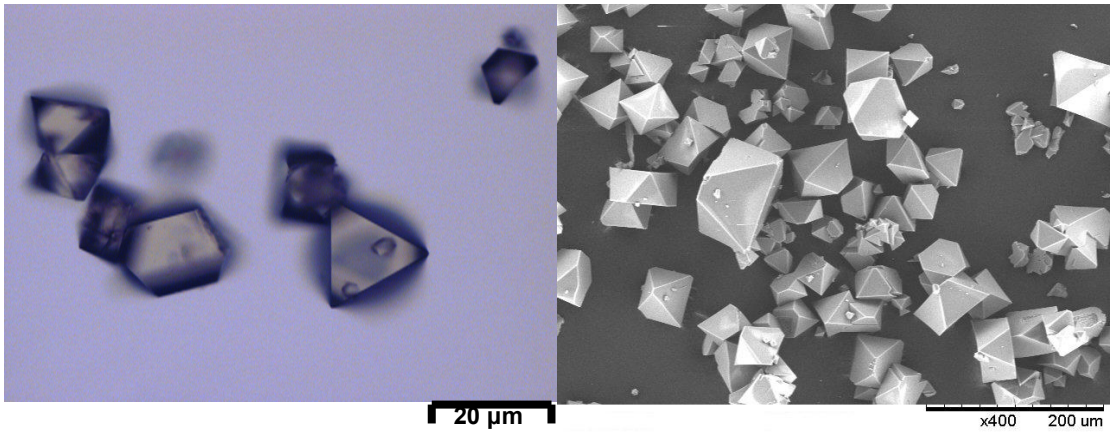

Fig. S2. Optical and scanning electron micrographs of compound **1**

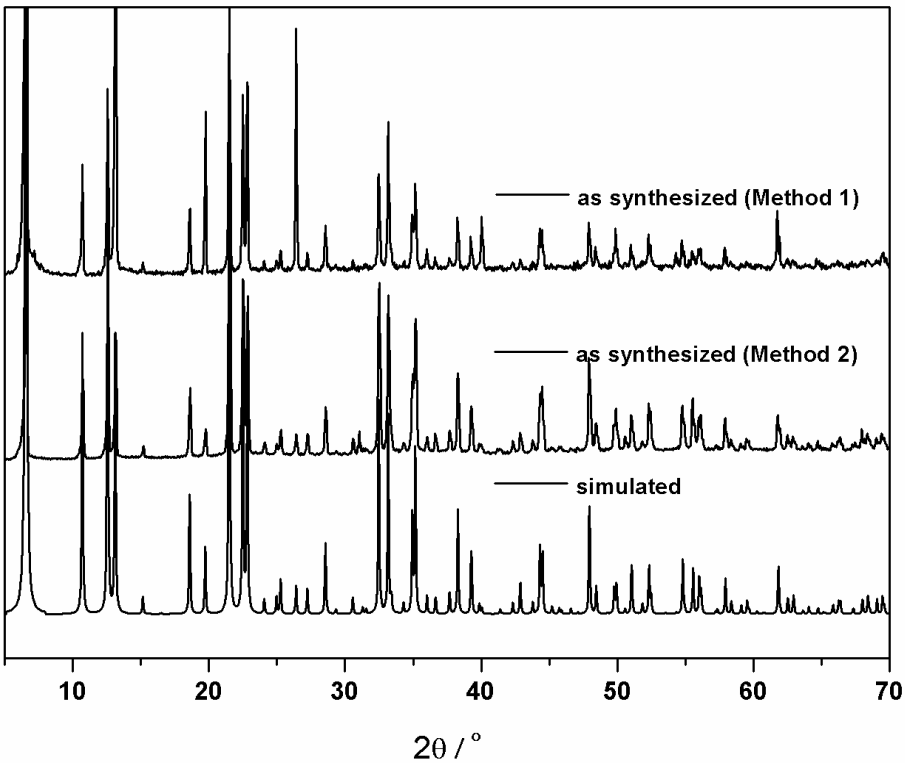

Fig. S3. Comparison of XRPD patterns of compound **1** (synthesized by two different methods) with a simulated XRPD pattern, as calculated from single crystal X-ray data.

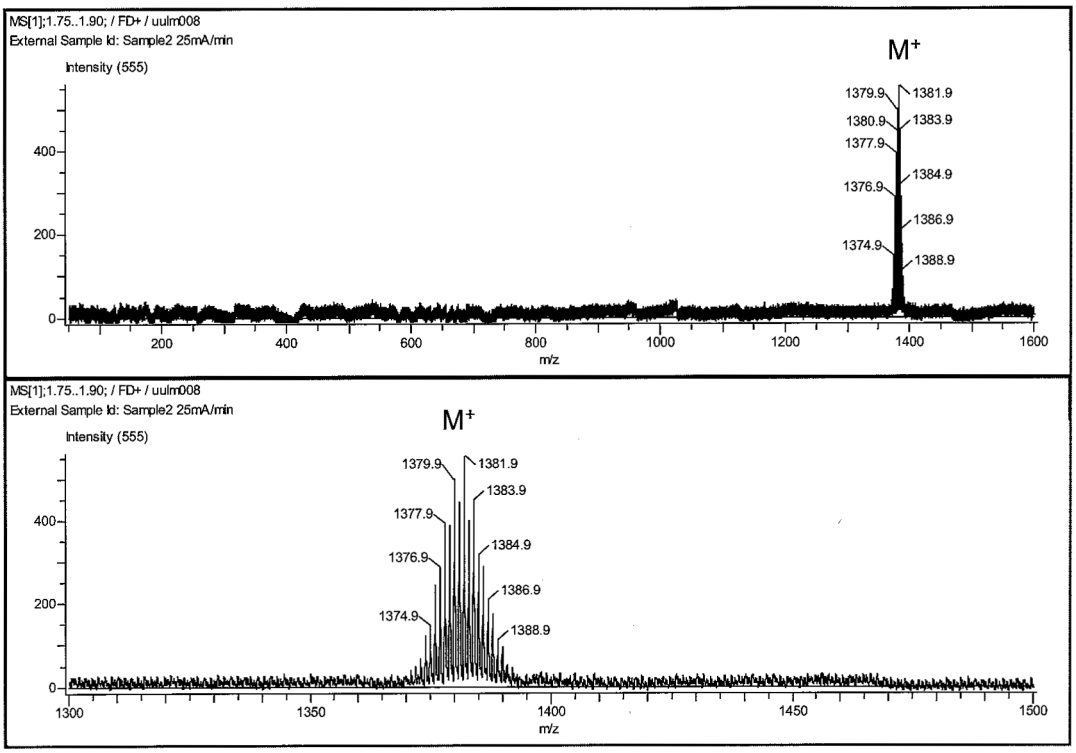

Fig. S4. (a) LIFDI mass spectrum of compound **1** (taken from an ethyl acetate solution) (Top: m/z 50-1600, bottom: m/z 1300-1500).

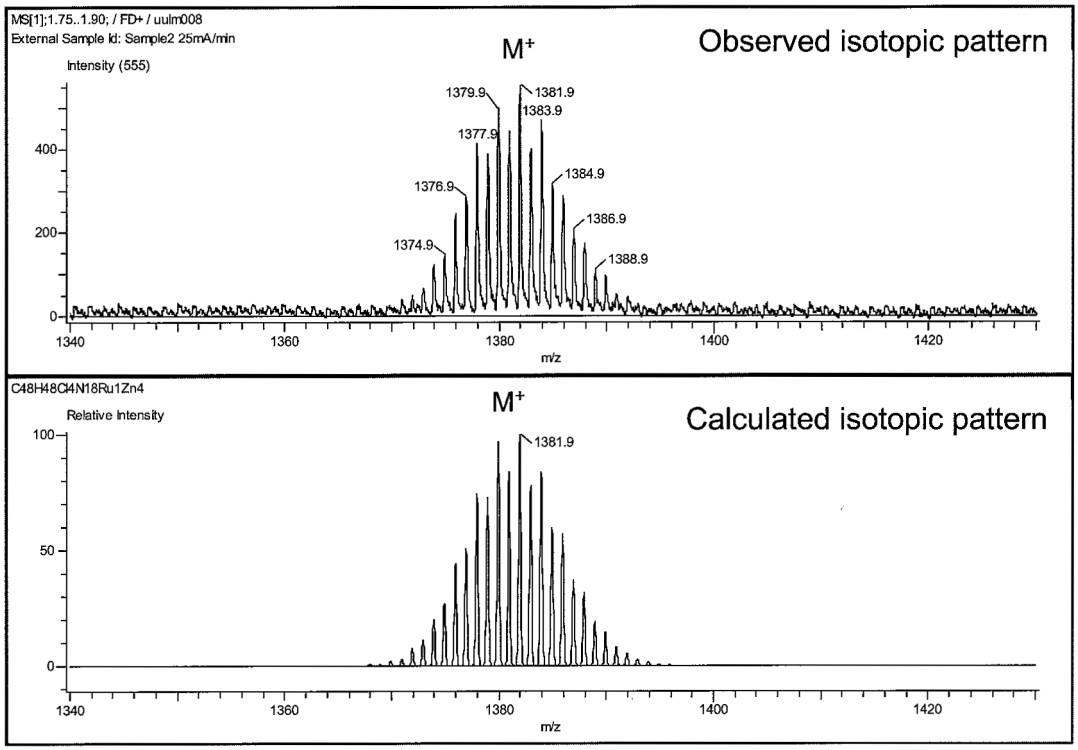

Fig. S4. (b) LIFDI mass spectrum of compound **1** (taken from an ethyl acetate solution)**.** Top: observed, bottom: calculated mass spectrum.

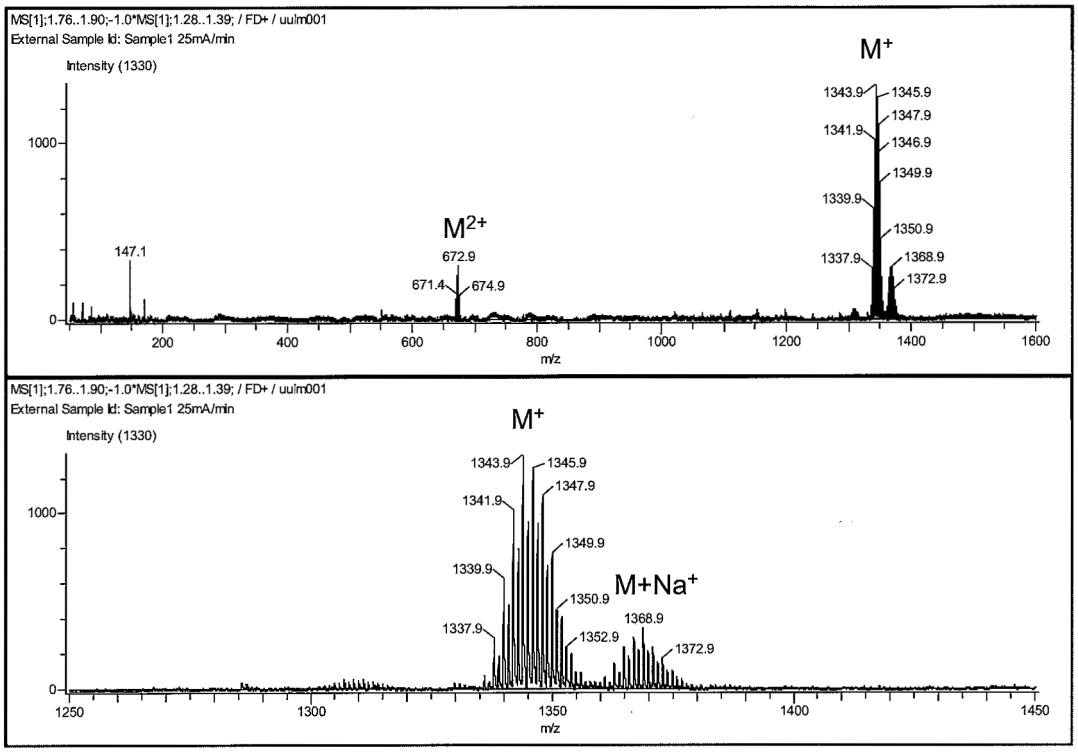

Fig. S5 (a). LIFDI mass spectrum of compound **2** (taken from an ethyl acetate solution)**.** (Top: m/z 50-1600, bottom: m/z 1250-1450).

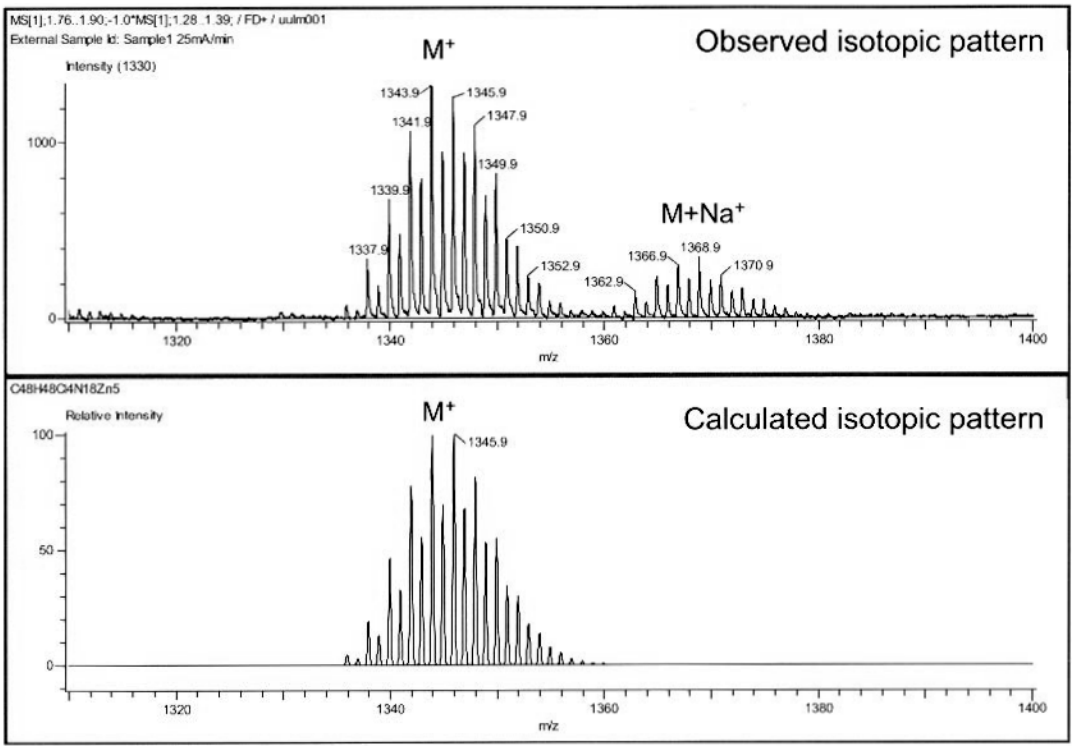

Fig. S5. (b) LIFDI mass spectrum of compound 2 (taken from an ethyl acetate solution). Top: observed, bottom: calculated mass spectrum.

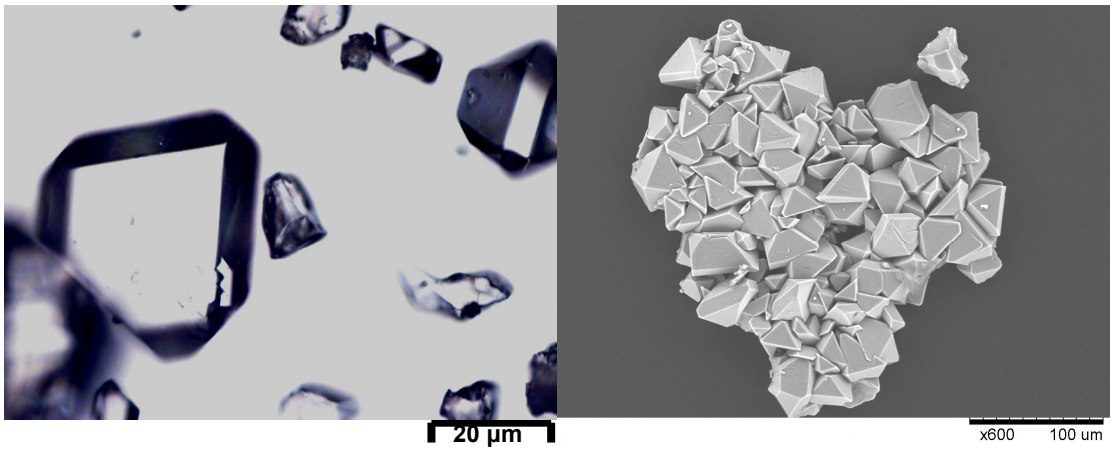

Fig. S6. Optical and scanning electron micrographs of compound **3**

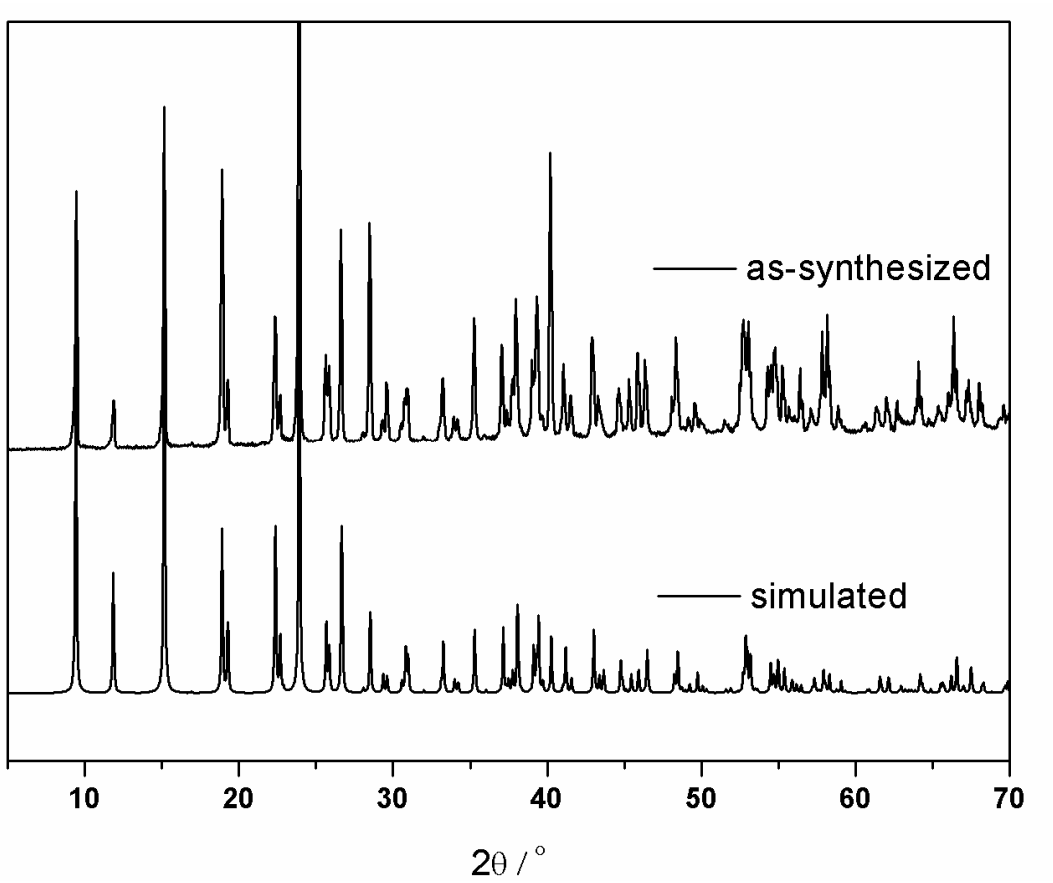

Fig. S7. Comparison of the experimentally observed XRPD pattern of compound **3** with a simulated XRPD pattern, as calculated from single crystal X-ray data..

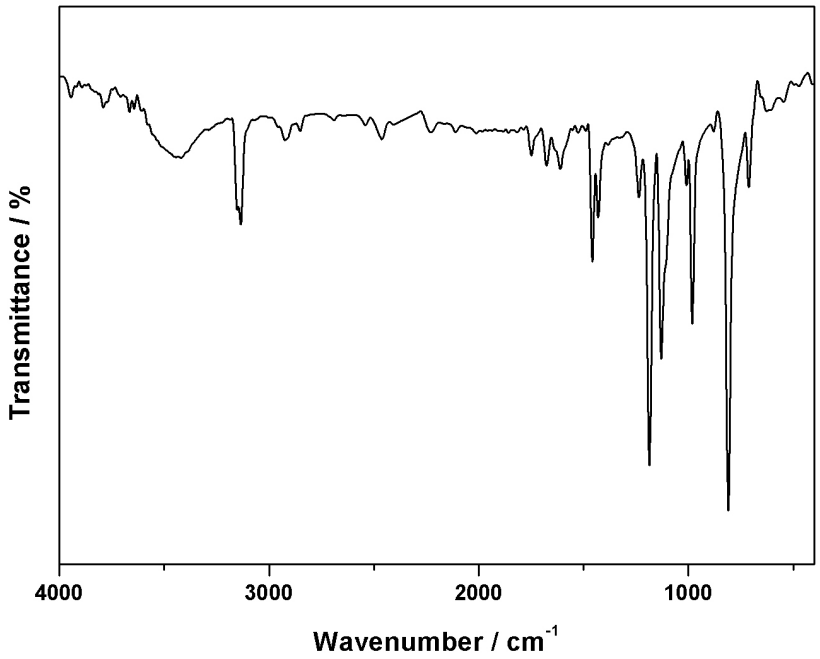

Fig. S8. FT-IR spectrum of $Zn_5Cl_4(ta)_6$ (**3**)

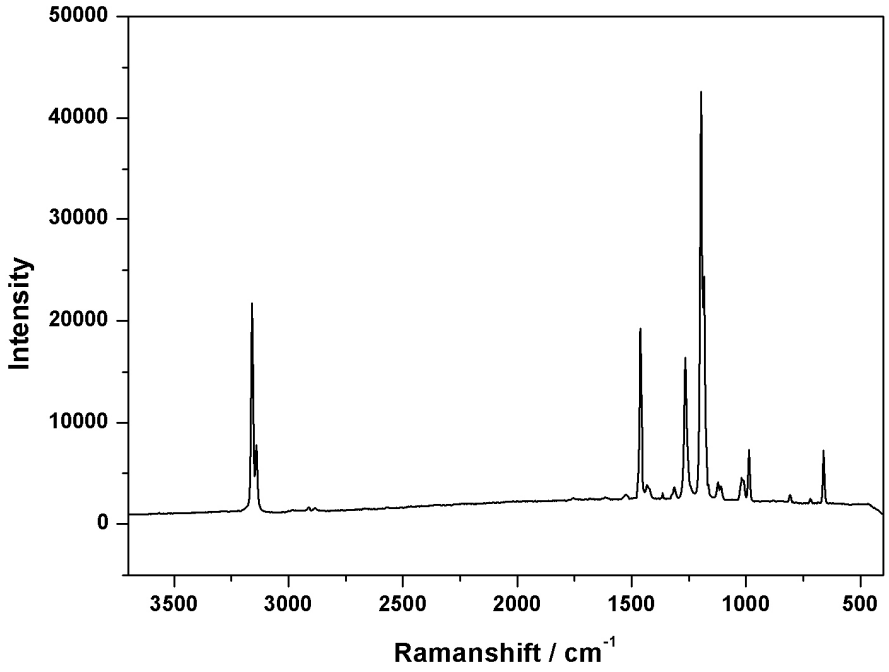

Fig. S9. Raman spectrum of $Zn_5Cl_4(ta)_6$ (**3**)

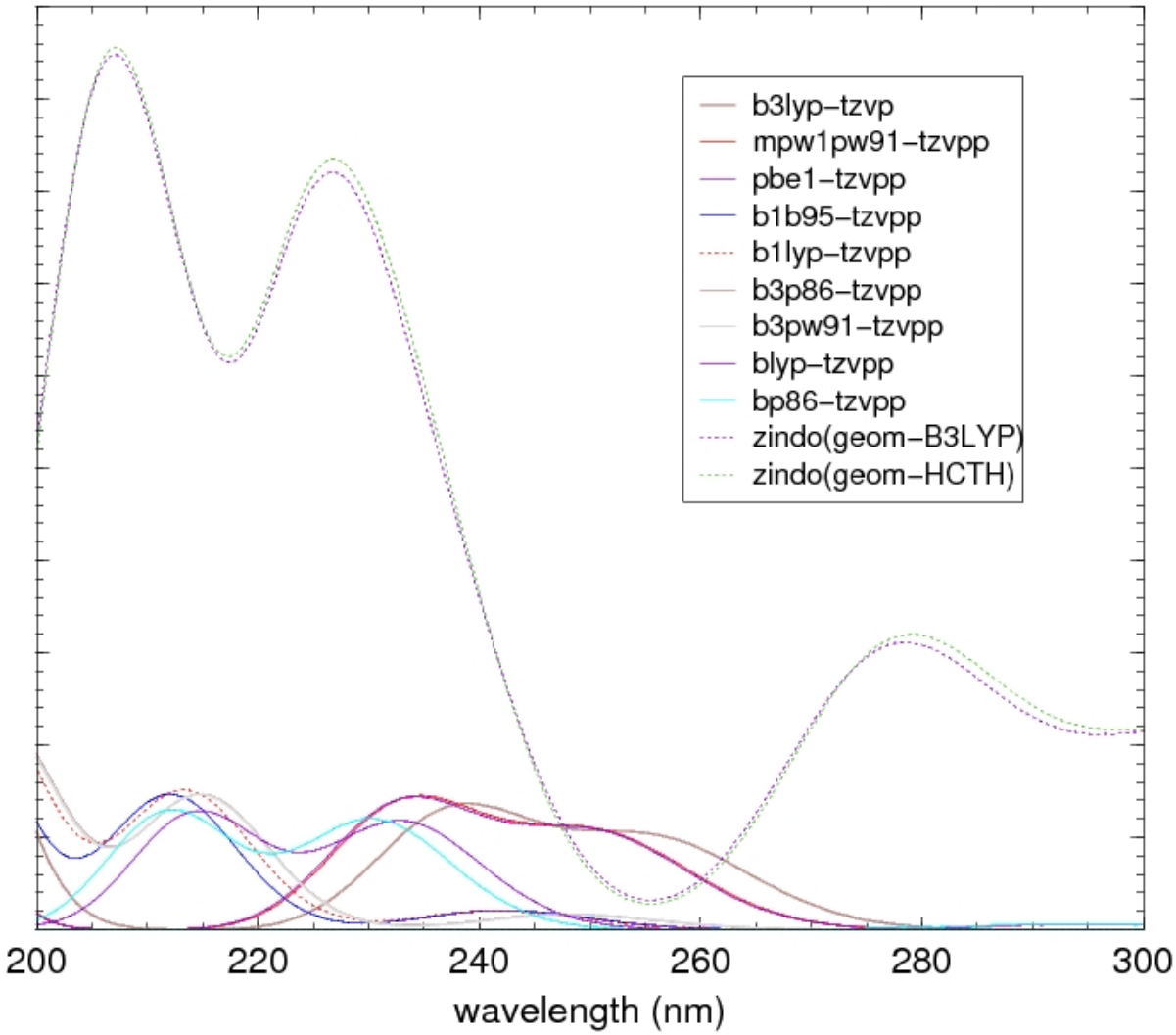

Fig. S10. UV-Vis spectra of btaH (1H-1,2,3-benzotriazole) as calculated by different methods: TDDFT (functionals and basis sets as specified) and ZINDO.

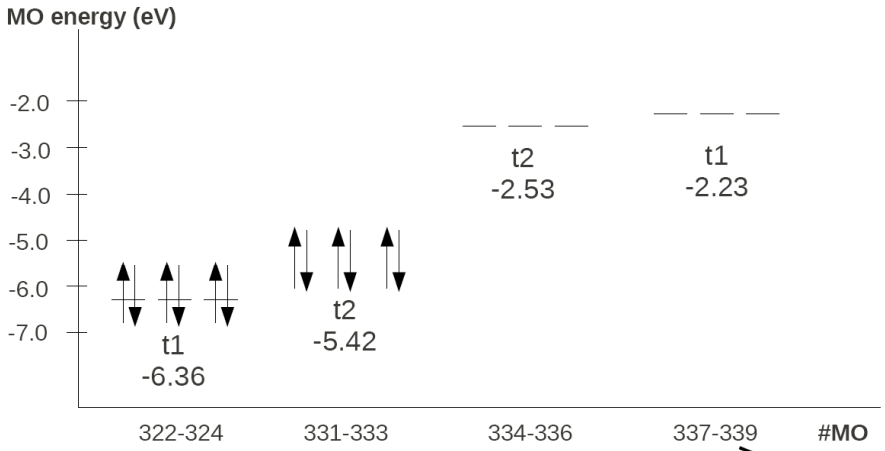

#HOMO = 333

Excited States (32 excitations calculated):

#	Sym	eV	nm	f	OM
15	$^1T_1$	3.13	395.8	0.378	{331-333}→{334-339}
16	$^1T_1$	3.13	395.8	0.390	{331-333}→{334-339}
17	$^1T_1$	3.15	393.9	0.527	{331-333}→{334-339}
31	$^1T_1$	4.32	287.1	0.963	{322-323}→{334-339}

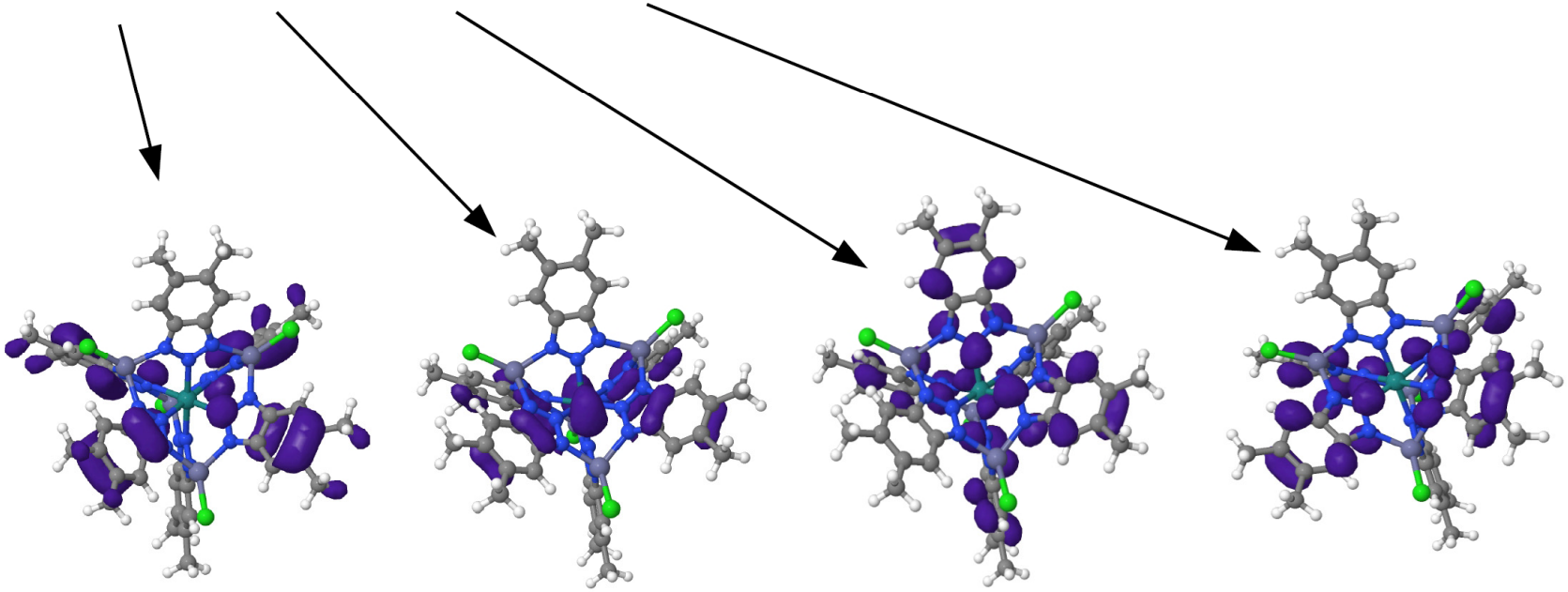

Fig. S11. Main components of the two bands in the UV-Vis spectrum of compound **1**, $[RuZn_4Cl_4(Me_2bta)_6]$ (cf. Fig. 11 in the manuscript). 'f' is the oscillator strength. The band at 393-396 nm is of MLCT type, whereas the band at 287 nm is a LLCT.

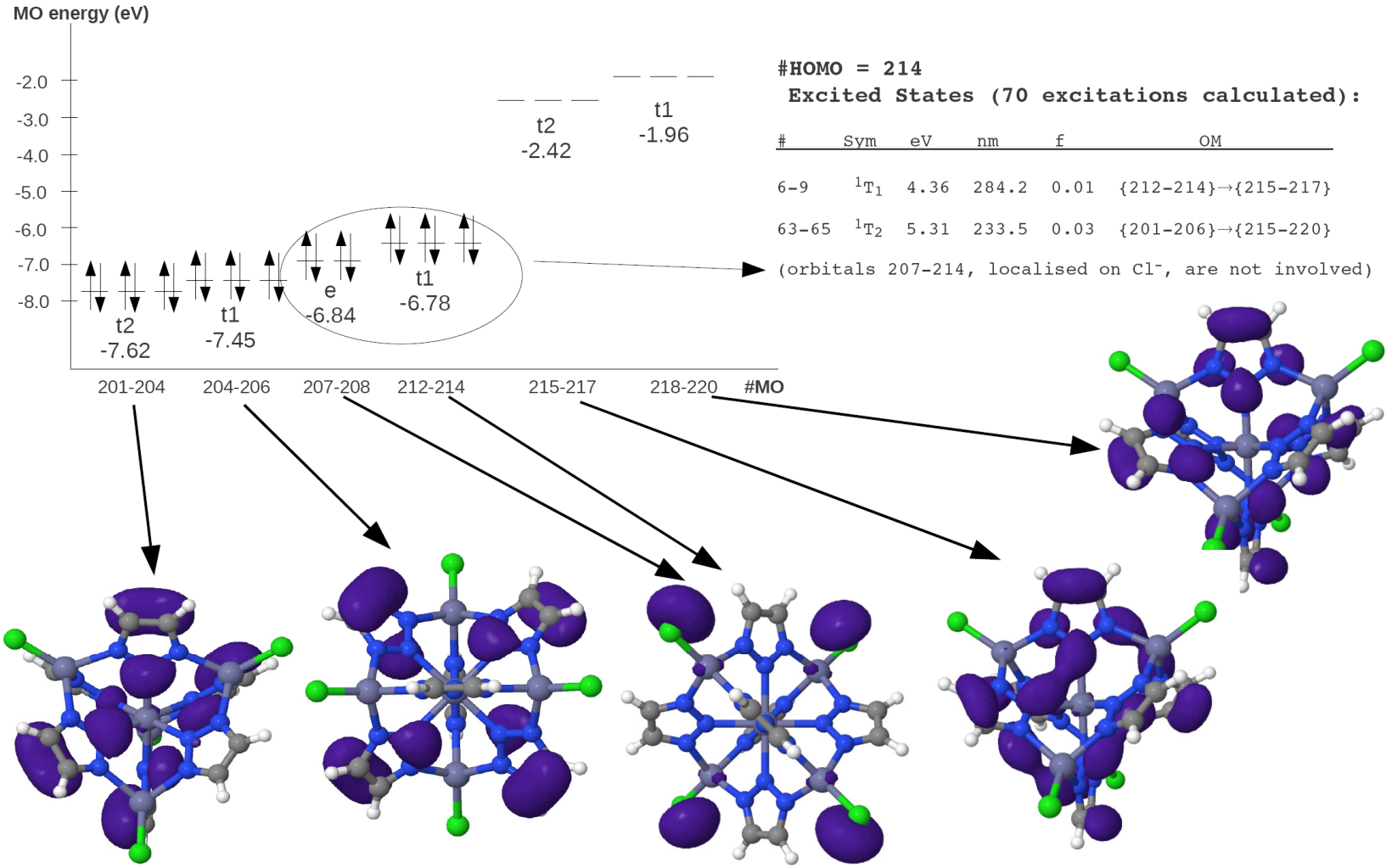

Fig. S12. Main components of the two bands in the UV-Vis spectrum of compound **3**, $[Zn_5Cl_4(ta)_6]$ (cf. Fig. 11 in the manuscript). 'f' is the oscillator strength. The bands at 284 and 233 nm are of LLCT type.

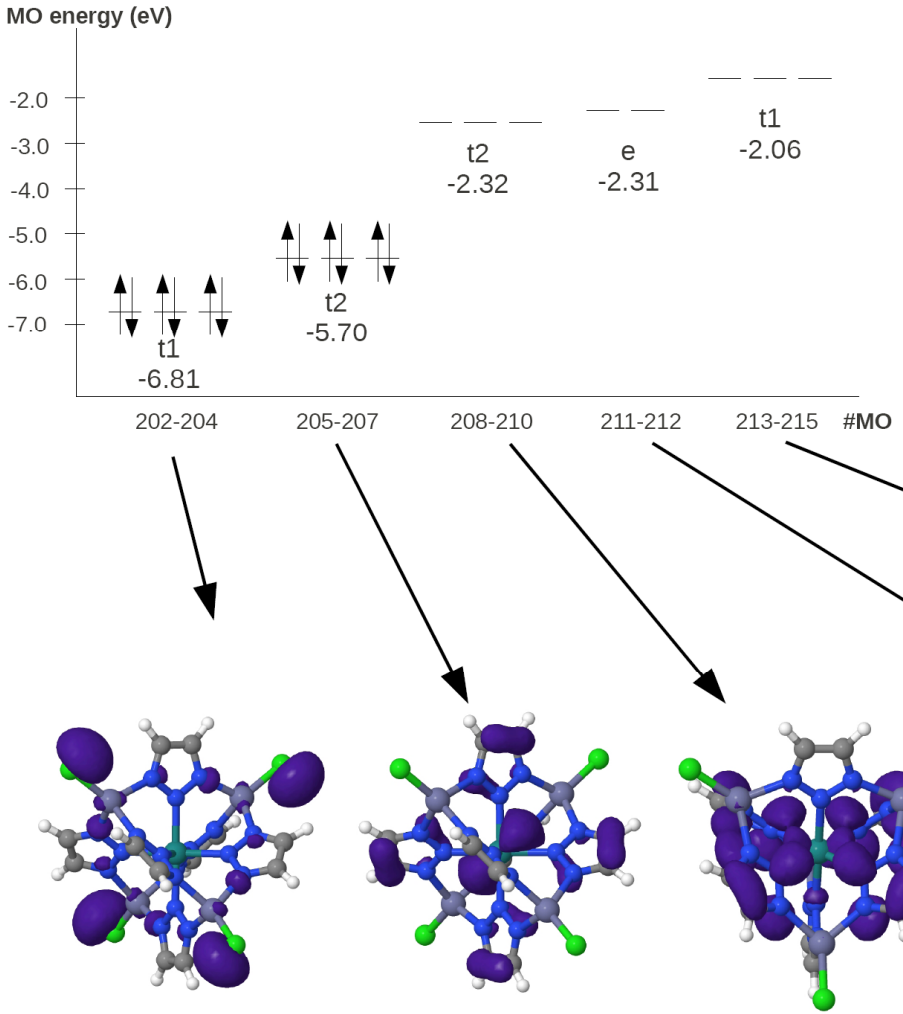

#HOMO = 207

Excited States (40 excitations calculated):

#	Sym	eV	nm	f	OM
6-8	$^1T_2$	3.48	356.5	0.075	{205-207}→{208-215}
18-20	$^1T_1$	3.78	327.9 329.1	0.396	{205-207}→{208-215}
30-32	$^1T_1$	4.50	275.7	0.009	{202-204}→{208-210}

Fig S13. Main components of the two bands in the UV-Vis spectrum of **3-Ru**, $[RuZn_4Cl_4(ta)_6]$ (cf. Fig. 11 in the manuscript). 'f' is the oscillator strength. The bands at 357 and 328 nm are of d-d and MLCT type whereas the band at 276 nm is a LLCT involving the Cl ligands.

Table S1. UV/Vis and steady-state fluorescence spectroscopic data of the three compounds

Samples	abs. λ_{max} (nm)	Emission, λ_{max} (nm)	Excitation, λ_{max} (nm)	Quantum Yield	τ (ns)	Photostability/ τ (ns)	
						before kinetic scan	after kinetic scan
From solution (Acetonitrile)							
Me_2btaH	264, 282	337(λ_{exc}=260)	281, 290(λ_{emi} =337)	1.90%	1.76(93.66%),5.04(6.34%)	1.74(81.41%), 5.03(18.59%)	0.47(5.10%), 2.44(65.41%), 4.58(29.49%)
(2)	282	356(λ_{exc}=287)	-	68.40%	2.11(3.1%),6.05(96.9%)	3.78(10.87%), 6.05(89.13%)	1.26(17.85%), 3.42(54.00%), 8.13(28.14%)
(1)	282, 335	310(λ_{exc}=250); 345(λ_{exc}=273) TRES solution	280(λ_{emi}=310)	1.80%	2.9(20.63%),7.61(79.37%)	4.22(52.66%), 10.12(42.04%), 1.07(5.3%)	4.36(54.31%), 10.60(37.73%), 1.02(7.95%)
Powdered form							
Me_2btaH	-	350(λ_{exc}=260)	-	-	0.23(93.66%), 5.04 (6.34%)	-	
(2)	-	364(λ_{exc}=287); 461(λ_{exc}=350)	-	-	0.14(9.76%), 2.65(88%), 6.57(2.24%); for 2nd emi. 0.35(4.9%), 3.33(75.12%), 6.2(19.98)	-	
(1)	-	317(λ_{exc}=260)	276(λ_{emi}=322)	-	316.7(2.72%), 2350(17.56%), 17400(79.7%)	-	

Sample: Me_2btaH: 5,6-Dimethyl-1H-benzotriazole; **(2):** $[Zn_5Cl_4(Me_2bta)_6]\cdot 2DMF$; **(1)**: $[Ru^{II}Zn_4Cl_4(Me_2bta)_6]\cdot 2DMF$

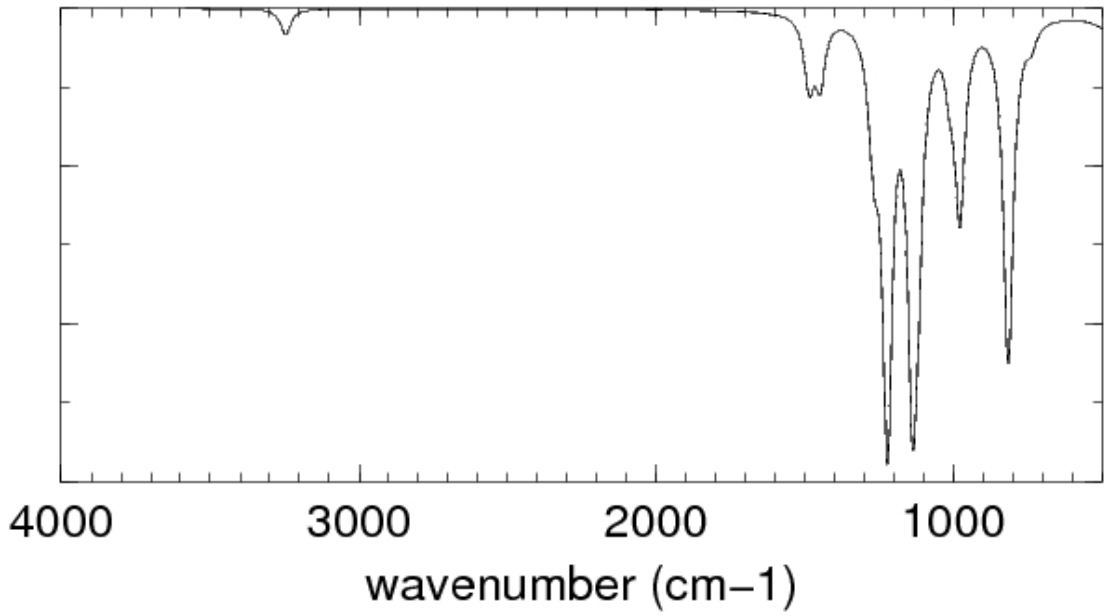

Fig. S14. DFT (HCTH-TZVPP) calculated infrared spectrum of (**3**). Compare to **Fig. S8**. The main features are: 815 (CH out of plane), 978 (ta skeleton, CCN bending), 1138 (HCN bending), 1222 (ZnN asym. stretching), 1448 (CN stretching or HCN bending), 1485 (C=C stretching) and 3245 (CH stretching).

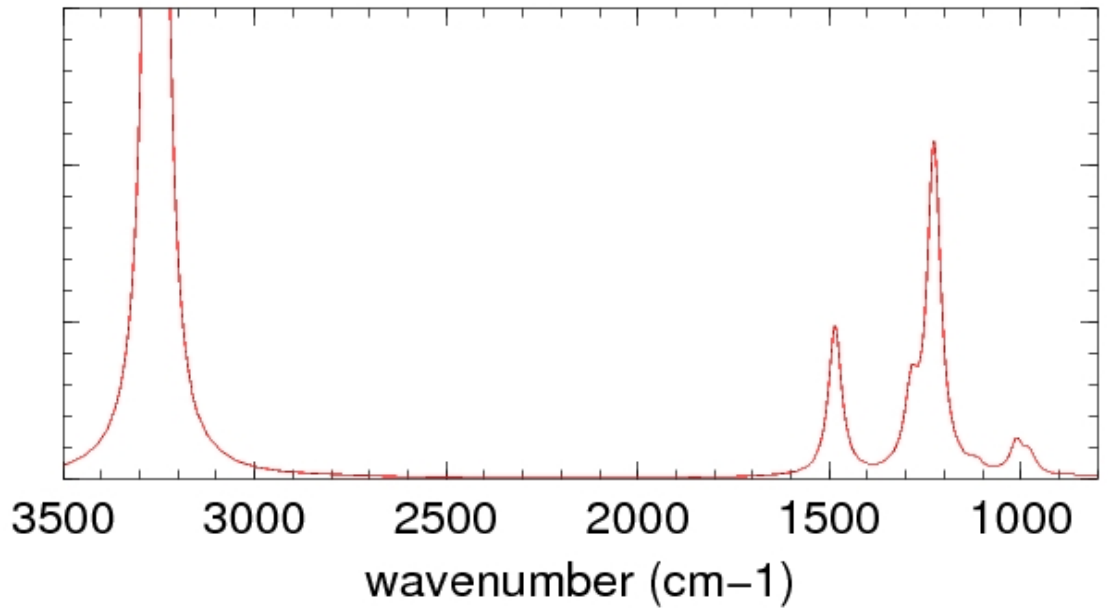

Fig. S15. DFT (HCTH-TZVPP) calculated Raman spectrum of (**3**), which gives as main active bands: 1011 (HCN bending), 1226 (ZnN stretching), 1281 (CN stretching), 1486 (CC stretching) and 3263 (CH stretching). Compare to **Fig. S9**.

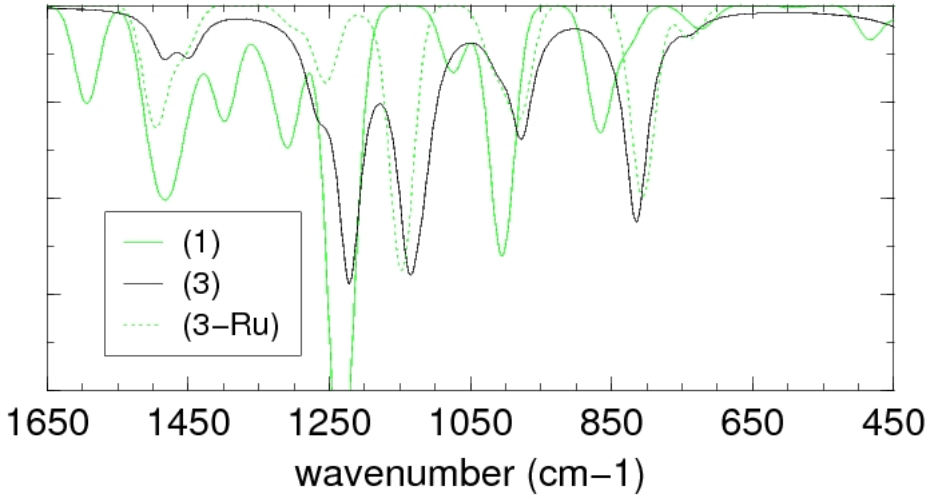

Fig. S16. Comparative features of DFT (HCTH-TZVPP) calculated infrared spectra of compounds **1**, **3** and **3-Ru**.

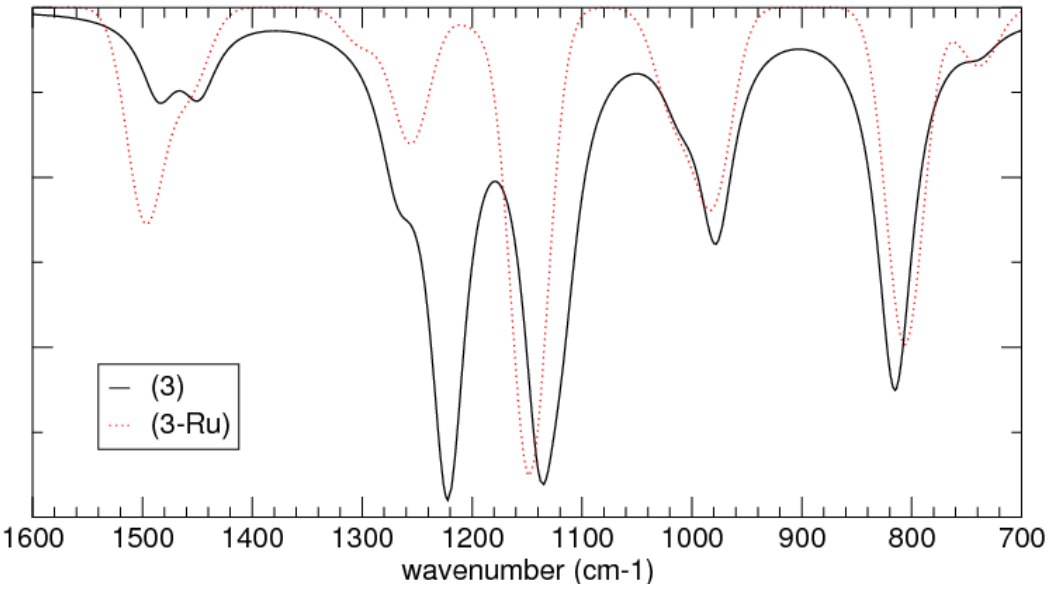

Fig. S17. Comparative features of DFT (HCTH-TZVPP) calculated infrared spectra of compounds **3** and **3-Ru**. Top and bottom figures have different scales of intensity.

Table S2. Active normal vibrational modes in the infrared spectra of compounds **3** and **3-Ru**, as calculated from DFT (HCTH-TZVPP). See **Figs. S16** and **S17**.

(**3**) (calc) (cm^{-1})	**Assignation**	(**3-Ru**) (calc) (cm^{-1})
	ZnCl stretching	50
	ClZnN bending	51
	Frame	163
	RuN stretching	216
230	ZnN asymmetric stretching	247
359	ZnCl stretching	
	NNZn bending	380
738	NNN out of plane	739
815	HCN out of plane	806
980	NCC bending	983
1010	HCX asymmetric bending	1010
1136	HCC symmetric bending	1148
1223	ZnN stretching	
1260	NN asymmetric stretching HCC bending	1255
1450	CN stretching	
1485	CC stretching HCN bending	1497
3248	CH asymmetric stretching	3250

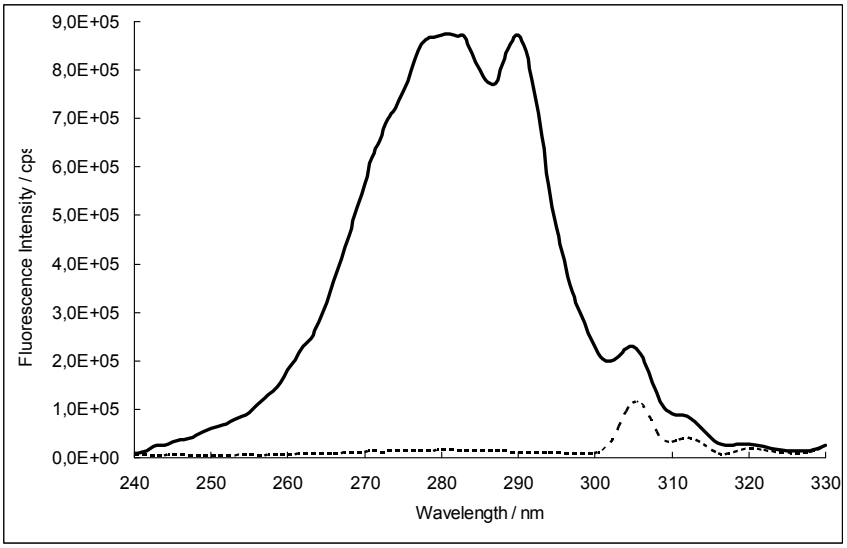

Fig. S18. Fluorescence excitation spectra of Me_2btaH in acetonitrile solution (—) and acetonitrile reference (····)

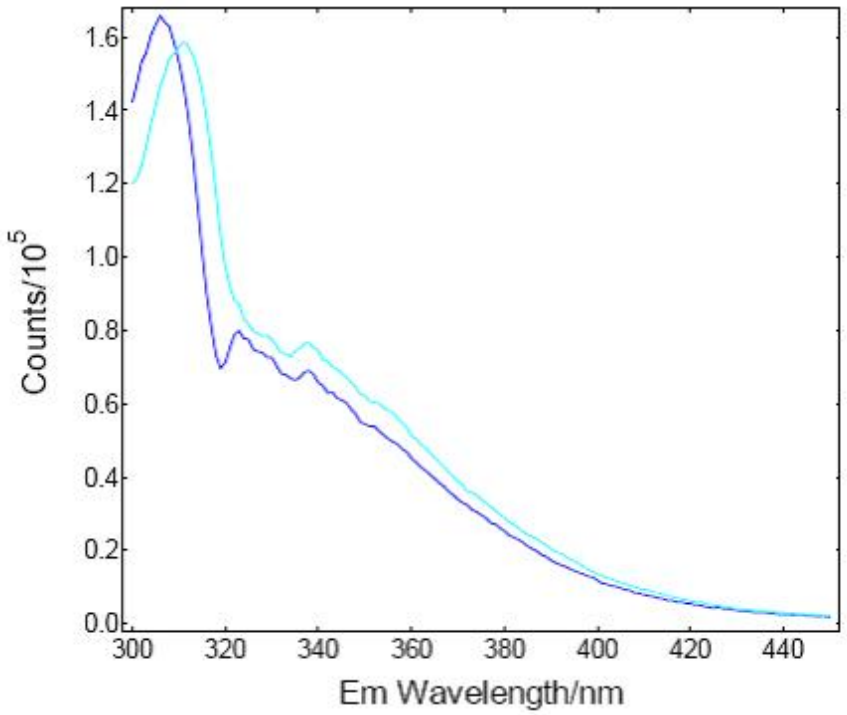

Fig. S19. Raman signals swamping the emission spectra of compound **1** (light blue, $\lambda_{EXC.}$=284nm, dark blue, $\lambda_{EXC.}$=280nm).

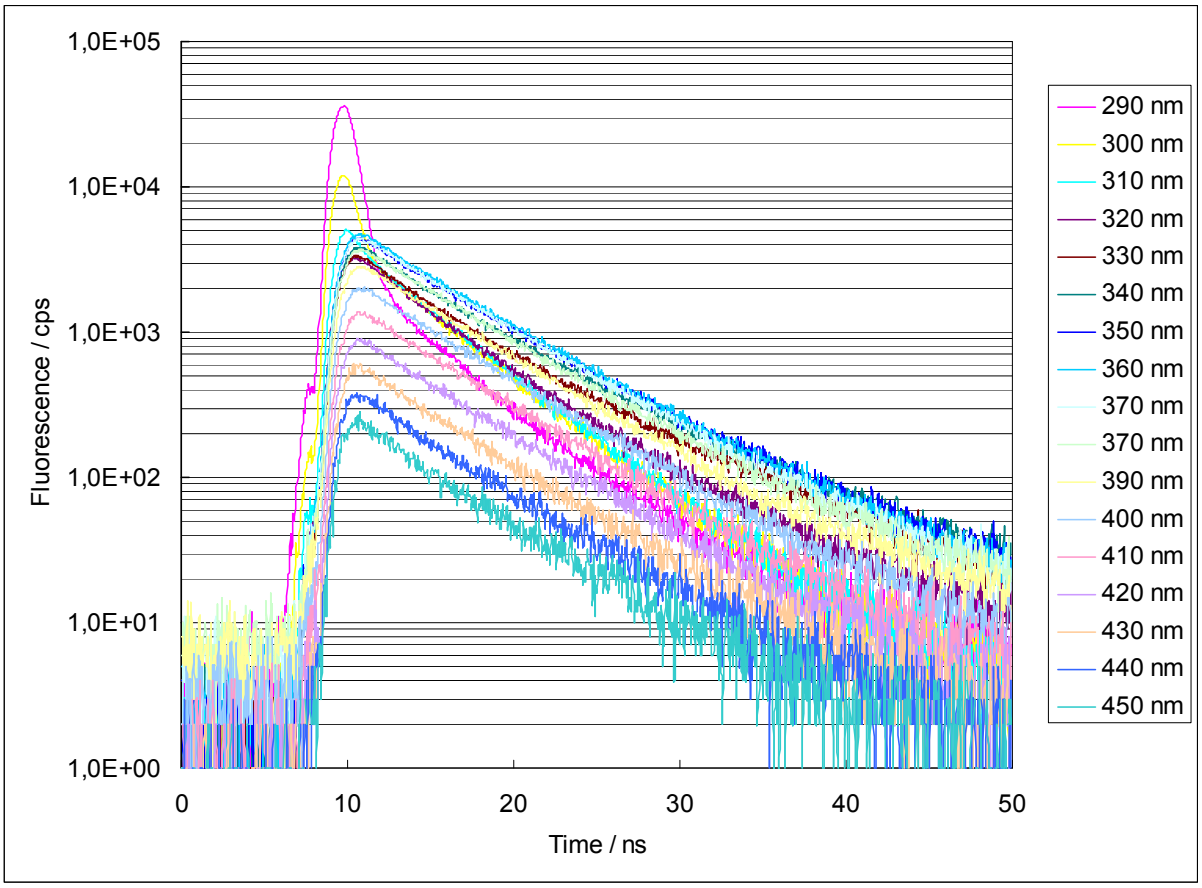

Fig. S20. TRES (Time Resolved Emission Spectrum) of **1**, $\lambda_{EXC.}$ = 273nm

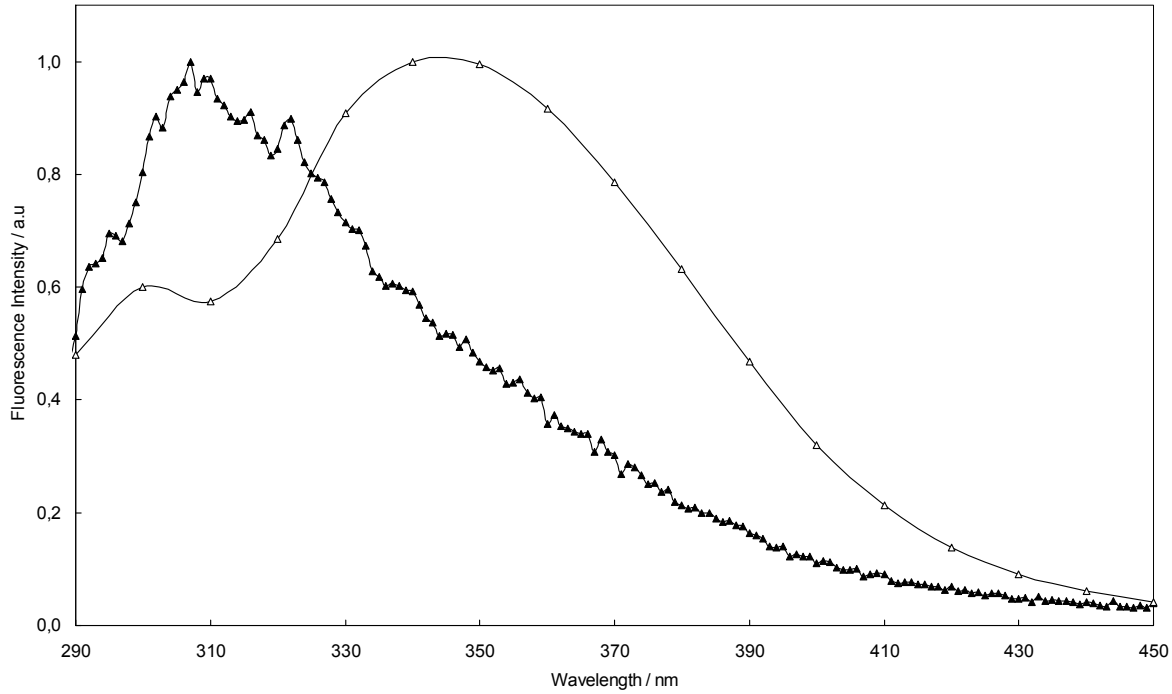

Fig. S21. Steady-state emission (▲,$\lambda_{EXC.}$=250 nm) and quasi-steady-state (△,λ_{EXC}=273 nm) spectra of compound **1**.

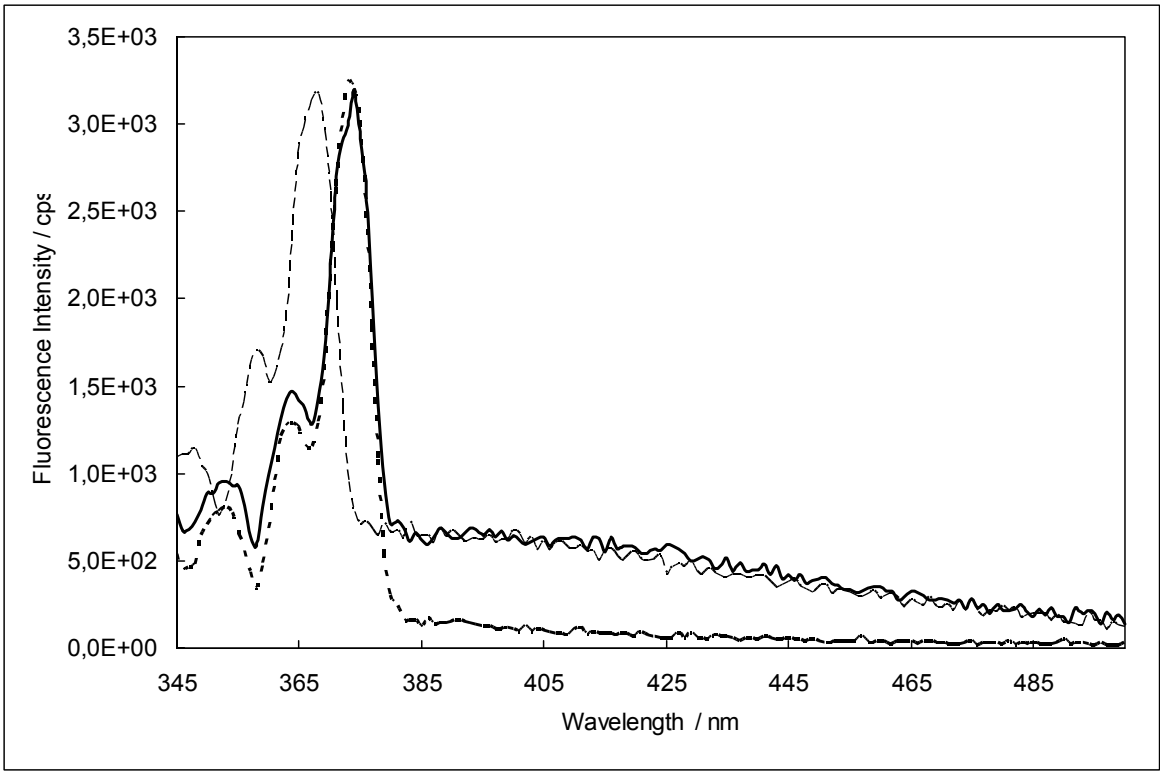

Fig. S22. Steady-state spectra of acetonitrile ($\lambda_{EXC.}$=335 nm, ····), **1** in acetonitrile, ($\lambda_{EXC.}$=330, ----), **1** in acetonitrile ($\lambda_{EXC.}$= 335 nm, —)

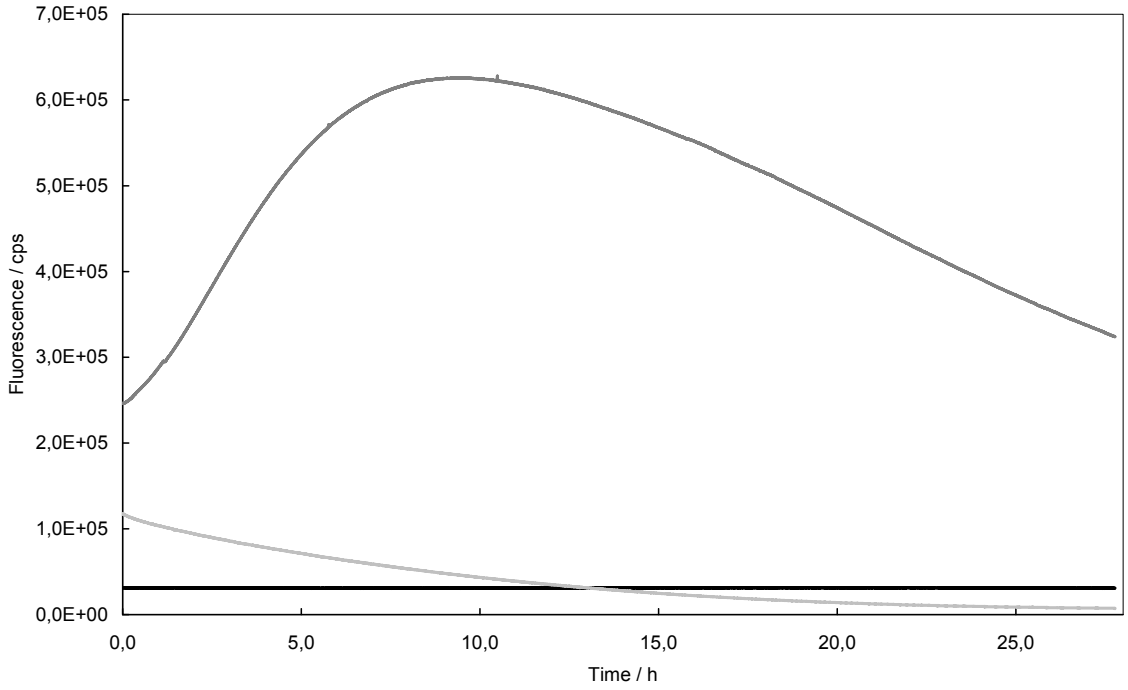

Fig. S23. Kinetic scan of **1** (black), **2** (light grey) and Me_2btaH (dark grey).

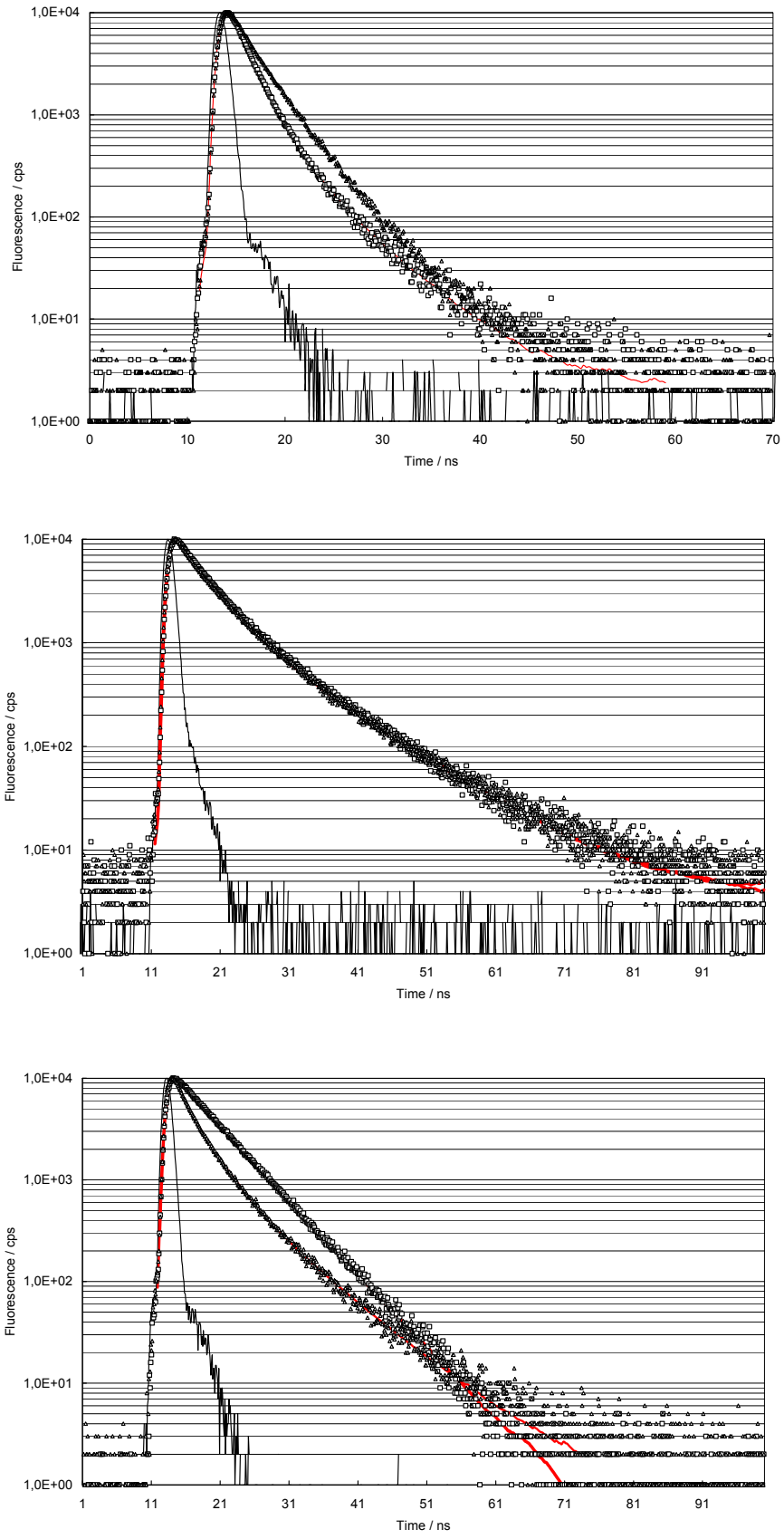

Fig. S24. Fluorescence decays of Me_2btaH (top), **1** (middle) and **2** (bottom) before (☐) and after (△) photobleaching. IRF (—), Fit (—), $\lambda_{EXC.}$=280nm,

Table S3. Experimental Conditions of steady-state and lifetime measurements of **1**

	Measurement	**$\lambda_{EXC.}$ (nm)**	**Excitation bandpass (nm)**	**$\lambda_{EMI.}$ (nm)**	**Emission Bandpass (nm)**
Solution	Steady-state excitation scan	250-295	2	310	10
Solution	Steady-state emission scan	250	10		2
Solution	Lifetime	273	11	340	15
Solution	Quantum Yield	282	1		1
Powder	Steady-state excitation scan	250-300	2	322	10
Powder	Steady-state emission scan	260	8		5
Powder	Lifetime	273	11	380	10

Table S4. Experimental conditions of steady state and lifetime measurements of **2**

	Measurement	**$\lambda_{EXC.}$ (nm)**	**Excitation bandpass (nm)**	**$\lambda_{EMI.}$ (nm)**	**Emission Bandpass (nm)**	**λ_{MAX} (nm)**
Solution	Steady-state excitation scan	240-340	1	356	1	
Solution	Steady-state emission scan	287	1		1	
Powder	Steady-state excitation scan		1	364	1	
Powder	Steady-state emission scan	318	1		1	
Solution	Steady-state emission scan before bleaching	287	3		1	356
Solution	Steady-state emission scan after bleaching	287	3		1	335
Solution	Lifetime	273	11	356	5	
Powder	Lifetime	273	11	364	1	
Solution	Quantum yield	278	1	300-700	1	
Solution	Kinetic scan	287	15	356	0,5	
Solution	Lifetime before/after bleaching	280	11	356	5	

Table S5. Experimental conditions of all steady state measurements of Me_2btaH**.**

	Measurement	**$\lambda_{Exc.}$ (nm)**	**Excitation bandpass (nm)**	**$\lambda_{Emi.}$ (nm)**	**Emission Bandpass (nm)**	**$\lambda_{MAX,}$ (nm)**
Solution	Steady-state excitation scan		1	350	5	281, 290
Powder	Steady-state excitation scan		5		1	310
Solution	Steady-state emission scan	260	5		1	337
Solution	Steady-state emission scan before bleaching	280	15		1	336
Solution	Steady-state emission scan after bleaching	280	15		1	308
Powder	Steady-state emission scan	260	5		1	353
Solution	Lifetime	273	11	350	10	
Powder	Lifetime	273	11	350	3	
Solution	Quantum Yield	273	5		1	
Solution	Kinetic scan	280	15	335	3	
Solution	Lifetime before/ after bleaching	280	11	335	5	